JOURNAL OF SOLID STATE CHEMISTRY **124,** 322–328 (1996)
ARTICLE NO. 0244

A Mixed-Valence Molybdenum Monophosphate with a Three-Dimensional Framework: $LiMo_2O_3(PO_4)_2$

S. Ledain, A. Leclaire, M. M. Borel, and B. Raveau

Laboratoire CRISMAT, CNRS URA 1318, ISMRA et Université de Caen, Bd du Maréchal Juin, 14050 Caen Cedex, France

Received November 13, 1995; in revised form April 4, 1996; accepted April 16, 1996

A new mixed-valence monophosphate possessing a unique structure type, $LiMo_2O_3(PO_4)_2$, has been synthesized. It crystallizes in the $P2_1/m$ space group with $a = 7.771$ (1) Å, $b = 12.687$ (2) Å, $c = 8.445$ (2) Å, $\beta = 106.94$ (1)°. Its three-dimensional $[Mo_2P_2O_{11}]_\infty$ framework consists of two kinds of $[Mo_2P_2O_{15}]_\infty$ chains. The first kind of chain running along [101] is built up from "Mo_2PO_{13}" units linked through single PO_4 tetrahedra; the second kind of chain, running along [100] is similar to that encountered in $W_2O_3(PO_4)_2$. This framework is also described by the three-dimensional assemblage of $[MoPO_8]_\infty$ chains, running along b. One recognizes two sorts of small tunnels running along b and a, respectively. The second kind of tunnel exhibits a similarity with that observed in the brownmillerite structure. Another novelty of this structure deals with the existence of two coordinations for lithium: tetrahedral and octahedral. The octahedral lithium ions obstruct the tunnels running along a and share two oxygen atoms with Mo(1) corresponding to the free vertices of the MoO_6 octahedra; the tetrahedral lithium ions share one oxygen atom with Mo(2), and one oxygen with Mo(3) corresponding to the free vertex of the $Mo(3)O_6$ octahedron.

INTRODUCTION

The recent investigations of the molybdenum phosphates of univalent A cations with the general formulation $A_xMo_2P_2O_{11}$ have shown the possibility to generate various novel structures. The nature of the $[Mo_2P_2O_{11}]_\infty$ framework seems to be closely related to the size and to the rate of the intercalated A cation. For the largest cations, such as rubidium or cesium, mixed-valence molybdenum monophosphates with a layer structure, $AMo_2O_3(PO_4)_2$ with A = Rb or Cs (1), are synthesized with two kinds of coordination for Mo (octahedral and trigonal bipyramidal). Increasing the content of univalent A cations allows an intersecting tunnel structure to be generated, built up from corner-linked octahedral Mo_2O_{11} dimers; the latter is obtained for the Mo(V) monophosphates α-$A_2O(MoO)_2(PO_4)_2$ with A = K, Rb, Tl, K/Cs, K/Rb, and Rb/Cs (2–5) and for $Cs_{1.5}O(MoO)_2(PO_4)_2$ (6). Potassium exhibits a second form with the same chemical composition but with a very different tunnel structure, built up of diphosphate groups and edge-linked octahedral Mo_2O_{10} dimers, and formulated β-$K_2O_2(MoO)_2P_2O_7$ (7). No anhydrous sodium phosphate with the formulation $Na_xMo_2P_2O_{11}$ is known to date, but there exists a hydrated monophosphate, $Na_3Mo_2P_2O_{11}(OH)\cdot 2H_2O$ with a layer structure (8). The introduction of lithium in the $[Mo_2P_2O_{11}]_\infty$ framework was also shown with the synthesis of the monophosphate $Li_xMo_2O_3(PO_4)_2$ that exhibits a tunnel structure (10), already observed for $Na_x(Mo, W)_2O_3(PO_4)_2$ (11). This phosphate differs from the other phosphates of univalent cations by the low lithium content ($x \approx 0.2$) that introduces much lower Mo(V) content. Owing to its size being much smaller than the other univalent cations and closer to molybdenum, lithium is susceptible to form more close packed structures. For the reason, the possibility to synthesize $Li_xMo_2P_2O_{11}$ compounds with higher lithium contents was investigated. We report herein on a new mixed valent molybdenum monophosphate $LiMo_2O_3(PO_4)_2$ with a novel three-dimensional framework, where lithium exhibits two kinds of coordination, octahedral and tetrahedral.

EXPERIMENTAL

Single crystals of this new phosphate were grown from a mixture of nominal composition $LiMo_2P_2O_{11}$. This synthesis was performed in two steps, using adequate ratios of MoO_3, Mo, $H(NH_4)_2PO_4$, and Li_2CO_3 to obtain the above formulation. First a mixture of MoO_3, $H(NH_4)_2PO_4$, and Li_2CO_3 was ground in an agate mortar and heated in air to 673 K in a platinum crucible to eliminate CO_2, NH_3, and H_2O. In a second step, the appropriate amount of molybdenum metal was added and the finely ground mixture was sealed in an evacuated silica ampoule, and then heated for 32 h at 873 K, cooled 3 K per hour to 773 K, and finally quenched to room temperature. In the resulting mixture, the major phase occurred as black crystals with a minor phase as $LiMo_3P_3O_{16}$. The microprobe analysis of the black crystals leads to a Mo/P ratio (1/1) in agreement

0022-4596/96 $18.00

TABLE 1
Summary of Crystal Data, Intensity Measurements, and Structure Refinement Parameters for $LiMo_2P_2O_{11}$

Crystal data		
Space group	$P2_1/m$	
Cell dimensions	a = 7.771(1) Å	
	b = 12.687(2) Å	β = 106.94(1)°
	c = 8.445(2) Å	
Volume (Å)^3	796.4(2) Å^3	
Z	4	
ρ_{calc} (gcm^3)	3.644	
Intensity measurements		
λ(Mo$K\alpha$)	0.71073	
Scan mode	$\omega-\theta$	
Scan width (°)	1.2 + 0.35 tn θ	
Slit aperture (mm)	1.1 + tn θ	
Max θ(°)	45	
Standard reflections	3 measured every 3600 s	
Measured reflections	7024	
Reflections with $I > 3\sigma$	4788	
μ(mm^{-1})	3.61	
Structure solution and refinement		
Parameters refined	182	
Agreement factors	R = 0.021	R_w = 0.023
Weighting scheme	$w = 1/\sigma$	
Δ/σ max	<0.005	

with the formula $LiMo_2P_2O_{11}$ deduced from the structure determination.

Attempts to prepare a pure phase in the form of polycrystalline powder samples led always to a mixture of this new phase and other compounds such as $LiMo_3P_3O_{16}$ (9).

Structure Determination

A black crystal with dimensions 0.077 × 0.205 × 0.102 mm^3 was selected for the structure determination. The cell parameters were determined by diffractometric techniques at 294 K with a least square refinement based upon 25 reflections in the range $18 < \theta < 22$. The data were collected with a CAD4 Enraf Nonius diffractometer with the parameters reported in Table 1. The systematic extinctions $k = 2n + 1$ for $0k0$ are consistent with the space groups $P2_1/m$ and $P2_1$. The presence of $0\nu0$ Harker peaks in the Patterson function allowed the centrosymmetrical space group $P2_1/m$ to be chosen. The reflections were corrected for Lorentz and polarization effects and for absorption. The structure was solved by the heavy atom method. The refinement of the atomic parameters and the anisotropic thermal factors for Mo, P, and O atoms were successful in the space group $P2_1/m$. Subsequent Fourier synthesis allowed the Li atoms to be located. The refinement of the atomic coordinates and their anisotropic thermal parameters for Mo, P, O and isotropic thermal factor for lithium led to $R = 0.021$ and $R_w = 0.023$ and to the atomic parameters of Table 2. Due to the too high thermal parameters of Li(2), attempts to refine the occupancy of this site were made, but the occupancy factor remained equal to 1, in the range of σ.

Description of the Structure and Discussion

The projection of the $[Mo_2P_2O_{11}]_\infty$ framework along **b** (Fig. 1) reveals its three-dimensional character; the latter consists of corner-sharing PO_4 tetrahedra and MoO_6 octahedra, forming small tunnels running along **b**. In this rather close packed structure, each PO_4 tetrahedron shares its four vertices with MoO_6 octahedra, whereas each MoO_6 octahedron has one free vertex, and shares four vertices with PO_4 tetrahedra, and one vertex with another MoO_6 octahedron forming a Mo_2O_{11} octahedral dimer.

The $[Mo_2P_2O_{11}]_\infty$ framework can be described by the stacking along b of two kinds of $[Mo_2P_2O_{15}]_\infty$ layers, both built up from disconnected $[Mo_2P_2O_{15}]_\infty$ chains. The first kind of layer (Fig. 2) consists of $[Mo_2P_2O_{15}]_\infty$ chains running along [101]; the latter are built up from Mo_2PO_{13} units linked through PO_4 tetrahedra. Similar units have previously been observed for $Li_{0.2}Mo_2O_3(PO_4)_2$ (10) and $Na_x(Mo, W)_2O_3(PO_4)_2$ (11), linked also through PO_4 tetrahedra and forming disconnected $[Mo_2P_2O_{15}]_\infty$ chains

TABLE 2
Positional Parameters and Their Estimated Standard Deviations

Atom	x	y	z	B(Å^2)
Mo(1)	0.26914(2)	0.50167(1)	0.34685(2)	0.544(2)
Mo(2)	0.73405(2)	0.25	0.18343(2)	0.509(3)
Mo(3)	0.68447(3)	0.75	0.15937(2)	0.574(3)
P(1)	0.32191(7)	0.25	0.24728(8)	0.512(8)
P(2)	0.81388(5)	0.50820(3)	0.26200(5)	0.501(7)
P(3)	0.13911(7)	0.75	0.40511(8)	0.520(8)
Li(1)	0.5	0.5	0.	2.24(8)[a]
Li(2)	0.149(2)	0.25	0.472(2)	5.8(3)[a]
O(1)	0.3336(2)	0.5168(1)	0.1748(2)	1.26(3)
O(2)	0.5	0.5	0.5	0.91(3)
O(3)	0.2472(2)	0.6532(1)	0.3897(2)	1.05(2)
O(4)	0.2515(2)	0.3445(1)	0.3270(2)	0.94(2)
O(5)	0.0011(2)	0.5023(1)	0.2389(2)	0.94(2)
O(6)	0.1821(2)	0.4666(1)	0.5628(2)	1.18(2)
O(7)	0.9031(3)	0.25	0.1012(3)	2.30(6)
O(8)	0.5463(2)	0.25	−0.0212(2)	0.76(3)
O(9)	0.7065(2)	0.4079(1)	0.1946(2)	1.27(3)
O(10)	0.8974(2)	0.25	0.4247(2)	1.02(4)
O(11)	0.5244(2)	0.25	0.2940(2)	0.91(3)
O(12)	0.6350(3)	0.75	0.3404(2)	1.27(4)
O(13)	0.9558(2)	0.75	0.2739(2)	1.17(4)
O(14)	0.7014(1)	0.5926(1)	0.1419(2)	0.74(2)
O(15)	0.7615(2)	0.75	−0.0609(2)	1.12(4)

Note. Anisotropically refined atoms are given in the form of the equivalent isotropic displacement parameter defined as $B = (4/3)\sum_i\sum_j \mathbf{a}_i \cdot \mathbf{a}_j \cdot \beta_{ij}$.
[a] Atom isotropically refined.

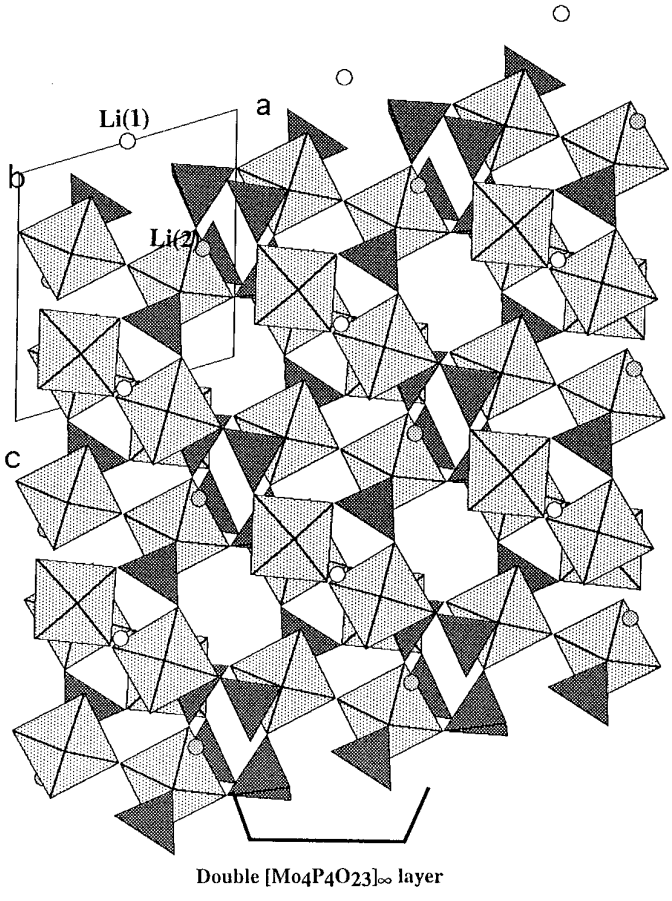

FIG. 1. Projection of the structure of $LiMo_2P_2O_{11}$ along **b**.

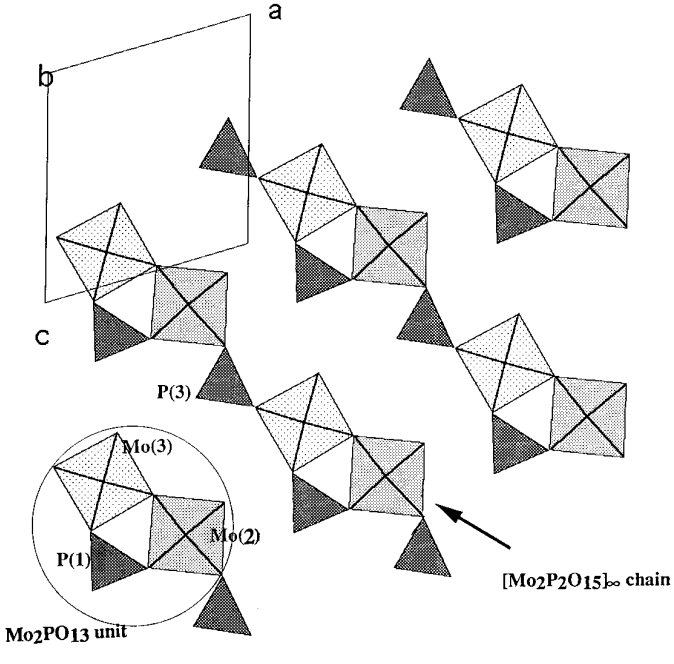

FIG. 2. The first kind of layer $[Mo_2P_2O_{15}]_\infty$ in $LiMo_2P_2O_{11}$.

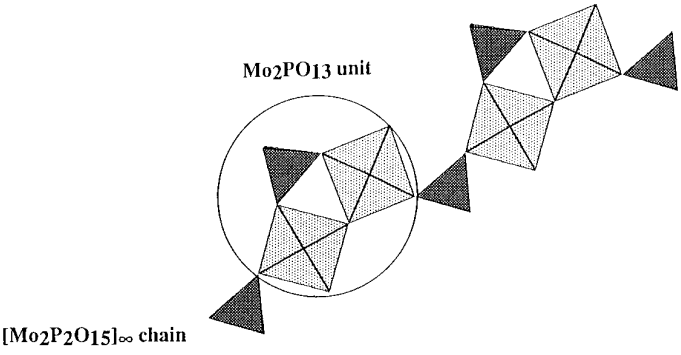

FIG. 3. The $[Mo_2P_2O_{15}]_\infty$ chain in $Li_{0.2}Mo_2O_3(PO_4)_2$ and $Na_x(Mo, W)_2O_3(PO_4)_2$ phosphates.

(Fig. 3); however the geometry of the chains is different in the two structures, due to the different orientations of the single PO_4 tetrahedra with respect to the Mo_2PO_{13} units. In the second kind of layer, the $[Mo_2P_2O_{15}]_\infty$ chains run along [100] (Fig. 4). The geometry of these chains is very similar to that observed for $W_2O_3(PO_4)_2$ (12). The latter tungsten oxyphosphate can indeed be described by the stacking of $[W_2P_2O_{15}]_\infty$ layers closely related to the second type of layers, built up from disconnected $[W_2P_2O_{15}]_\infty$ chains running along [100] (Fig. 5). The main difference between the layers of the two structures arises from the $[W_2P_2O_{15}]_\infty$ chains which are slightly translated with respect to each other leading to an angle of 106.9° for $Li(Mo_2O_3)(PO_4)_2$, against 91.9° for $W_2O_3(PO_4)_2$.

Thus, the $[Mo_2P_2O_{11}]_\infty$ three-dimensional framework of $LiMo_2O_3(PO_4)_2$ results from the stacking along **b** of such layers in such a way that the octahedra of one layer are connected to the tetrahedra of the next layer. In fact the periodicity along **b** corresponds to the stacking of four $[Mo_2P_2O_{15}]_\infty$ layers: starting with the stacking of one type I layer, and then one type II layer, the third layer belonging to type I but turned 180° with respect to the first, whereas the fourth layer is the enanthiomorph of the type II layer.

Such a stacking of the $[Mo_2P_2O_{15}]_\infty$ layers leads to the formation of $[MoPO_8]_\infty$ chains running along **b**, in which one MoO_6 octahedron alternates with one PO_4 tetrahedron (Fig. 6). In fact, the entire $[Mo_2P_2O_{11}]_\infty$ framework can also be described by the assemblage of such chains. Two types of chains can be distinguished according to the orientation of the PO_4 tetrahedra. In the first type of chains, the third vertices of the PO_4 tetrahedra are in the *cis* position with respect to the chain, whereas in the second type two successive PO_4 tetrahedra have their third vertices in the *trans* position (Fig. 6). The connection of these two kinds of chains alternatively forms $[Mo_2P_2O_{13}]_\infty$ layers parallel to (001). The latter exhibit two kinds of windows (Fig. 6): a small "V-shaped" window, and a longer "W-shaped" window. Two $[Mo_2P_2O_{13}]_\infty$ layers form double $[Mo_4P_4O_{23}]_\infty$

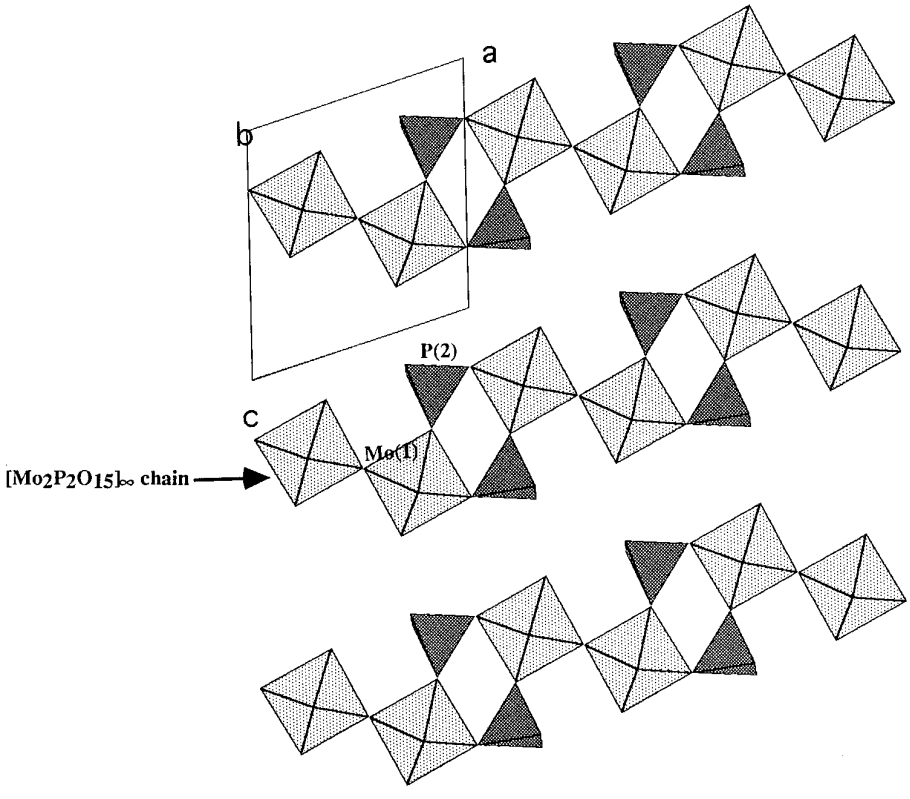

FIG. 4. The second kind of layer $[Mo_2P_2O_{15}]_\infty$ in $LiMo_2P_2O_{11}$.

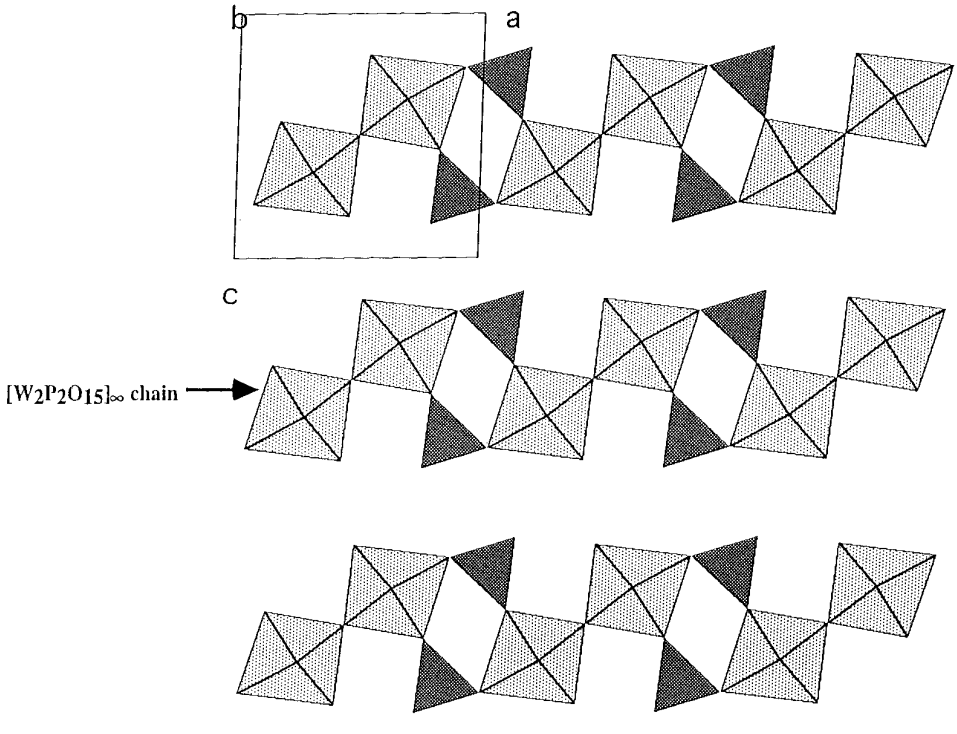

FIG. 5. The $[W_2P_2O_{15}]_\infty$ layer in $W_2O_3(PO_4)_2$.

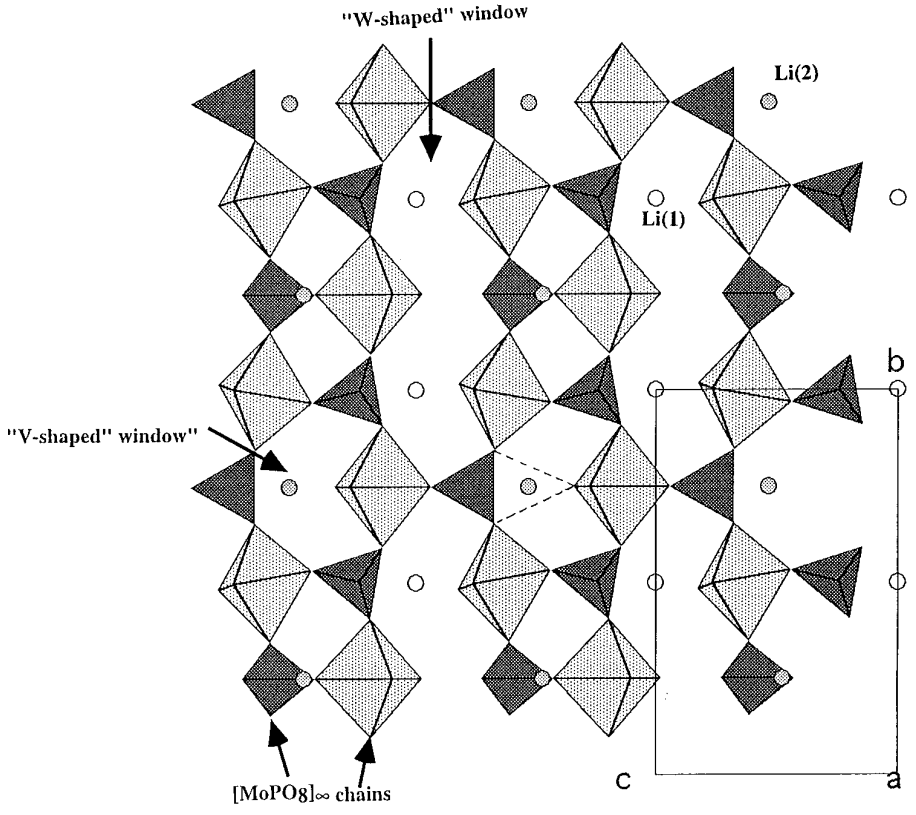

FIG. 6. $[MoPO_8]_\infty$ chains running along **b** showing "V" and "W" shaped windows.

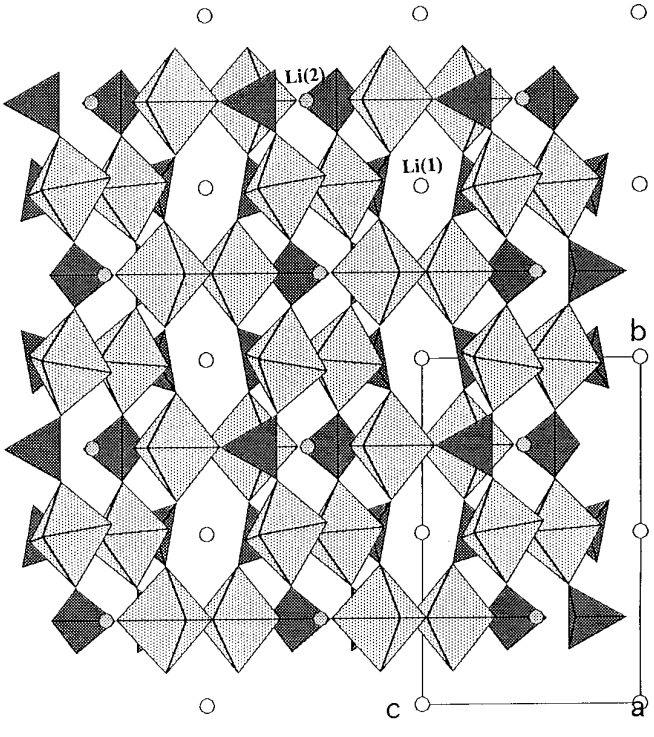

FIG. 7. Projection of the structure of $LiMo_2P_2O_{11}$ along **a** showing the six-sided tunnels.

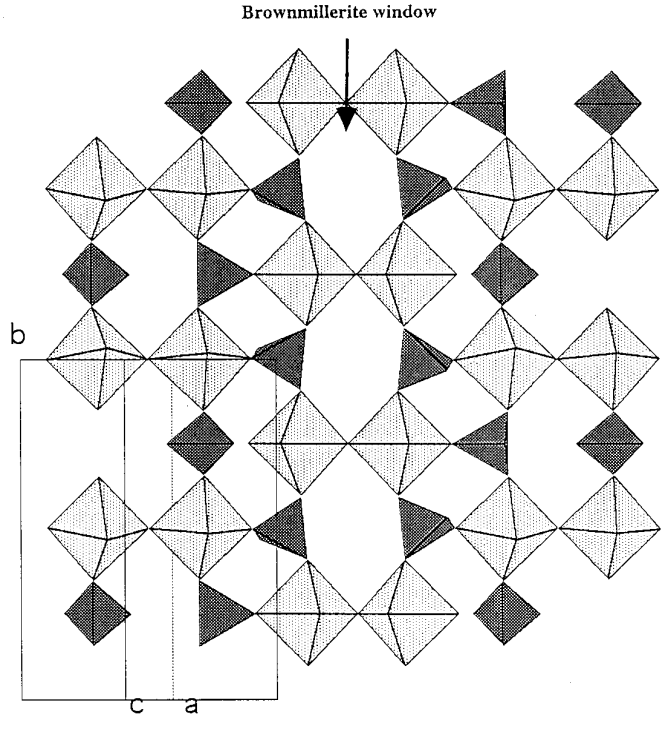

FIG. 8. The (101) layer of polyhedra in $LiMo_2P_2O_{11}$ showing the brownmillerite ribbon.

TABLE 3
Distances (Å) and Angles (°) in the Polyhedra

Mo(1)	O(1)	O(2)	O(3)	O(4)	O(5)	O(6)
O(1)	**1.680(2)**	2.681(1)	2.729(2)	2.705(2)	2.796(2)	3.844(2)
O(2)	97.53(5)	**1.881(3)**	2.727(1)	2.848(1)	3.861(1)	2.707(2)
O(3)	96.37(7)	90.06(3)	**1.973(1)**	3.953(2)	2.743(2)	2.903(2)
O(4)	94.12(7)	94.29(3)	168.03(6)	**2.002(1)**	2.739(2)	2.698(2)
O(5)	97.89(6)	164.52(4)	86.89(5)	85.96(5)	**2.016(1)**	2.725(2)
O(6)	174.60(6)	83.58(3)	88.91(6)	80.52(6)	81.19(5)	**2.168(2)**
Mo(2)	O(7)	O(8)	O(11)	O(9)	O(9)^{i}	O(10)
O(7)	**1.655(3)**	2.662(3)	3.755(3)	2.769(2)	2.769(2)	2.745(3)
O(8)	96.4(1)	**1.909(2)**	2.716(3)	2.750(2)	2.750(2)	3.955(2)
O(11)	178.50(9)	85.14(8)	**2.101(2)**	2.722(2)	2.722(2)	2.785(2)
O(9)	97.34(5)	88.79(4)	82.67(5)	**2.019(1)**	4.006(3)	2.883(2)
O(9)^{i}	97.34(5)	88.79(4)	82.67(5)	165.30(6)	**2.019(1)**	2.883(2)
O(10)	94.54(9)	169.10(8)	83.96(7)	89.82(4)	89.82(4)	**2.063(2)**
Mo(3)	O(12)	O(8)^{ii}	O(14)	O(14)^{iii}	O(13)	O(15)
O(12)	**1.682(2)**	2.653(3)	2.751(2)	2.751(2)	2.711(3)	3.794(3)
O(i)^{ii}	97.94(9)	**1.833(2)**	2.755(2)	2.755(2)	3.863(2)	2.678(3)
O(14)	95.97(4)	91.50(3)	**2.009(1)**	3.993(2)	2.802(2)	2.757(2)
O(14)^{iii}	95.97(4)	91.50(3)	167.16(6)	**2.009(2)**	2.802(2)	2.757(2)
O(13)	92.72(9)	169.35(9)	87.37(3)	87.37(3)	**2.048(2)**	2.790(3)
O(15)	176.92(8)	85.14(8)	83.91(4)	83.91(4)	84.20(8)	**2.114(2)**
P(1)	O(11)	O(15)^{iv}	O(4)	O(4)^{i}		
O(11)	**1.506(2)**	2.502(2)	2.521(2)	2.521(2)		
O(15)^{iv}	111.7(1)	**1.518(2)**	2.523(2)	2.523(2)		
O(4)	111.12(6)	110.61(7)	**1.551(2)**	2.398(2)		
O(4)^{i}	111.12(6)	110.61(7)	101.26(9)	**1.551(2)**		
P(2)	O(6)^{vi}	O(5)^{v}	O(9)	O(14)		
O(6)^{vi}	**1.505(2)**	2.525(2)	2.540(2)	2.507(2)		
O(5)^{v}	112.88(7)	**1.525(1)**	2.514(2)	2.509(2)		
O(9)	113.17(9)	110.33(8)	**1.538(1)**	2.384(2)		
O(14)	109.95(8)	109.00(8)	100.80(7)	**1.557(1)**		
P(3)	O(3)	O(3)^{iii}	O(13)^{vii}	O(10)^{viii}		
O(3)	**1.515(1)**	2.457(2)	2.511(2)	2.501(2)		
O(3)^{iii}	108.37(8)	**1.515(1)**	2.511(2)	2.501(2)		
O(13)^{vii}	111.13(7)	111.13(7)	**1.529(2)**	2.467(3)		
O(10)^{viii}	109.68(7)	109.68(7)	106.8(1)	**1.544(2)**		

Li(1)–O(1)	2.238(2)	Li(2)–O(4)	2.04(1)
Li(1)–O(9)	2.260(1)	Li(2)–O(10)^{vii}	1.88(1)
Li(1)–O(14)	2.043(1)	Li(2)–O(12)^{viii}	1.94(1)
Li(1)–O(1)^{ix}	2.238(2)	Li(2)–O(4)^{i}	2.04(1)
Li(1)–O(9)^{ix}	2.260(1)		
Li(1)–O(14)^{ix}	2.043(1)		

Symmetry codes
i: x; 1/2 − y; z
ii: 1 − x; 1/2 + y; −z
iii: x; 3/2 − y; z
iv: 1 − x; y − 1/2; −z
v: x + 1; y; z
vi: 1 − x; 1 − y; 1 − z
vii: x − 1; y; z
viii: 1 − x; 1 − y; −z
ix: 1 − x; y − 1/2; 1 − z

Note. The Mo–O or P–O distances are on the diagonal, above it are the O···O distances, and below are the O–Mo–O or O–P–O angles.

layers by sharing the vertices of their MoO_6 octahedra (see Fig. 1); the $[Mo_2P_2O_{11}]_\infty$ three-dimensional framework results from the stacking of the double $[Mo_4P_4O_{23}]_\infty$ layers that share the vertices of their MoO_6 octahedra and PO_4 tetrahedra.

The view of the structure along **a** (Fig. 7) shows the relationships between this structure and that of brownmillerite; one indeed recognizes the presence of six-sided tunnels where the lithium ions Li(1) are located with an octahedral coordination. In fact, the similarity with the brownmillerite structure is better seen by considering (101) layers of polyhedra (Fig. 8): one clearly observes brownmillerite ribbons running along **b**, built up from rings of four MoO_6 octahedra and two PO_4 tetrahedra.

In the $[Mo_2P_2O_{11}]_\infty$ framework, the PO_4 tetrahedra exhibit a regular configuration, with P–O distances ranging from 1.505 to 1.557 Å (Table 3), characteristic of the monophosphate groups. The three independent MoO_6 octahedra exhibit a geometry characteristic of Mo(V) (Table 3), with one very short Mo=O bond (1.65 to 1.68 Å) corresponding to the free vertex, one opposite longer bond (2.10 to 2.16 Å) and four intermediate Mo–O distances (1.83 to 2.06 Å). The bond valence calculations lead to the valences of 5.35 for Mo(1), 5.28 for Mo(2), and 5.41 for Mo(3), in agreement with the mean valence deduced from the formula (5.5). This suggests that the Mo(V) and Mo(VI) species are distributed randomly over the three sites, the geometry of the octahedra being imposed by the presence of Mo(V).

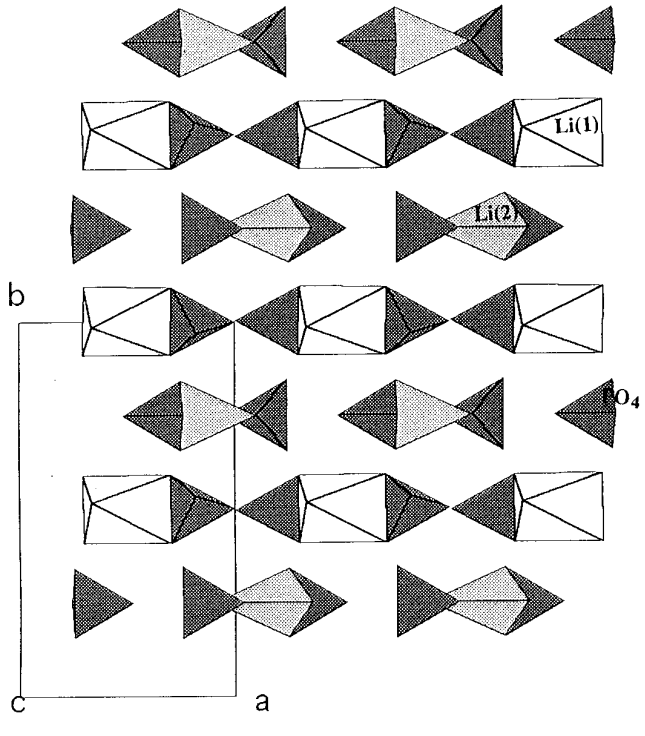

FIG. 9. The connection between the PO_4 tetrahedron and the lithium octahedra and tetrahedra. The MoO_6 octahedra are omitted.

The presence of lithium with both coordinations, tetrahedral and octahedral, is a novel feature of this structure. The Li(1) cation, which exhibits octahedral coordination, with Li–O distances ranging from 2.04 to 2.26 Å (Table 3), is located in the six-sided tunnels running along **a** (Fig. 7). In fact, in these tunnels each LiO_6 octahedron shares two opposite edges with two tetrahedra forming the brownmillerite window (Fig. 9) so that the tunnels are completely obstructed by the LiO_6 octahedra. The two remaining vertices of the LiO_6 octahedra correspond to the free vertices of the Mo(1) octahedra. The Li(2) cations exhibit a distorted tetrahedral coordination with Li–O distances ranging from 1.88 to 2.04 Å. These ions are located near the center of "V-shaped" window (Fig. 6) so that one LiO_4 tetrahedron shares one edge with one PO_4 tetrahedron one vertex with one Mo(2) octahedron, and the fourth vertex with the free corner of the Mo(3) octahedron.

This study shows the great ability of lithium, phosphorus, and molybdenum to form a mixed framework entirely built up from tetrahedra and octahedra. It suggests the possibility to generate other novel frameworks in the system Li–Mo–P–O, by varying the cationic ratios and the molybdenum mean valence.

REFERENCES

1. T. Hoareau, A. Leclaire, M. M. Borel, A. Grandin, and B. Raveau, *J. Solid State Chem.* **116,** 87 (1995).
2. G. Gueho, M. M. Borel, A. Grandin, A. Leclaire, and B. Raveau, *J. Solid State Chem.* **104,** 202 (1993).
3. A. Guesdon, A. Leclaire, M. M. Borel, A. Grandin, and B. Raveau, *Acta Crystallogr. Sect. C* **50,** 1852 (1994).
4. A. Guesdon, M. M. Borel, A. Grandin, A. Leclaire, and B. Raveau, *Acta Crystallogr. Sect. C* **49,** 1877 (1993).
5. A. Guesdon, A. Leclaire, M. M. Borel, and B. Raveau, *Eur. J. Solid State Inorg. Chem.* **33,** 385 (1996).
6. M. M. Borel, A. Leclaire, A. Grandin, and B. Raveau, *J. Solid State Chem.* **108,** 336 (1994).
7. A. Guesdon, A. Leclaire, M. M. Borel, A. Grandin, and B. Raveau, *J. Solid State Chem.* **114,** 481 (1995).
8. L. A. Mundi and R. Haushalter, *Inorg. Chem.* **29,** 2879 (1990).
9. T. Hoareau, M. M. Borel, A. Leclaire, J. Provost, and B. Raveau, *Mater. Res. Bull.* **18,** 523 (1995).
10. S. Ledain, A. Leclaire, M. M. Borel, and B. Raveau, *J. Solid State Chem.* **122,** 107 (1996).
11. A. Leclaire, M. M. Borel, J. Chardon, and B. Raveau, *J. Solid State Chem.* **120,** 353 (1996).
12. P. Kierkegaard, *Acta Chem. Scand.* **14,** 657 (1960).